WARSAW UNIVERSITY OF TECHNOLOGY Index 351733
FACULTY OF CIVIL ENGINEERING
COMMITTEE FOR CIVIL AND WATER ENGINEERING
POLISH ACADEMY OF SCIENCES ISSN 1230-2945

DOI: 10.24425/ace.2024.149866

ARCHIVES OF CIVIL ENGINEERING

Vol. LXX ISSUE 2 2024

pp. 323 –342

Research paper

Mechanical properties of polymer fibre reinforced concrete in the light of various standards

Julia Blazy[1], Łukasz Drobiec[2], Paweł Wolka[3]

Abstract: The article presents the results of a detailed experimental campaign including a compressive strength test, three- and four-point bending test (3PBT and 4PBT, respectively) of polymer fiber reinforced concrete with the addition of metakaolin. The comprehensive analysis included three Types of concrete mixture differing in amount and used polymer fibers. It was concluded that polymer fibers did not influence the maximum compressive and flexural tensile strength of concrete. On the other hand, they had a beneficial effect on the ductility, residual and equivalent flexural tensile strengths, and fracture energy of samples. The mixtures of Type 1 and 2 were characterized by softening behaviour but the mixture of Type 3 by soft-hardening behaviour. In the 3PBT, the residual flexural tensile strengths obtained according to EN 14651 did not correspond clearly with equivalent flexural tensile strengths calculated in compliance with RILEM TC 162-TDF. It is noteworthy that the effectiveness and correctness of equations presented in other work of the authors referring to dependencies between deflection, crack and tip mouth opening displacements for the 3PBT were confirmed on samples with different composition and fibers. Based on the 4PBT, the equivalent flexural tensile strengths according to JCI-SF4 standard were calculated and the correlations with the results from 3PBT were defined.

Keywords: concrete drainage channel, fiber reinforced concrete, four-point bending test, polymer fiber, three-point bending test

[1]M.Sc. Eng., Silesian University of Technology, Faculty of Civil Engineering, Akademicka 5, 44-100 Gliwice, Poland, e-mail: julia.blazy@polsl.pl, ORCID: 0000-0001-9525-8650
[2]Prof., DSc., PhD., Eng., Silesian University of Technology, Faculty of Civil Engineering, Akademicka 5, 44-100 Gliwice, Poland, e-mail: lukasz.drobiec@polsl.pl, ORCID: 0000-0001-9825-6343
[3]PhD., Eng., Astra Technologia Betonu sp. z o.o., 83-010 Straszyn, Poland, e-mail: pawel@astra-polska.com, ORCID: 0000-0001-7921-720X

1. Introduction

Nowadays, there is an increasing emphasis on the development of concrete responsible production and consumption [1–3]. This is because cement production is responsible for about 5% of global CO_2 emissions. Namely, the carbon footprint amounts to around 0.710, 0.571, 0.405, 0.473, and 0.485 tons of CO_2 per 1 ton of CEM I, CEM II, CEM III, CEM IV, and CEM V production, respectively [4]. The European Cement Association CEMBUREAU aims to reduce the emissions noted for 1990 by as much as 40% by 2030, while 3% of this reduction would be possible thanks to the decrease of clinker/cement ratio by the use of other materials such as silica fume, fly ash, granulated blast furnace slag or metakaolin [5]. In Europe, in 2017, cement contained 77% of clinker, which means that around 23% of clinker was replaced with alternative materials. Until 2030 CEMBUREAU plans to increase this replacement to 26% [5]. Other possibilities following the low-emission concrete idea are connected with the optimization of a concrete mixture: production of new types of cement, improvement of the cement grinding process, usage of recycled concrete, increase of aggregates' packing in concrete; usage of emission-neutral energy and transport; and attention to thermal efficiency (modernization of furnaces and investment in the heat recovery). Last but not least approach refers to the Carbon Capture and Usage/Storage (CCUS) technology which has been researched for several years [6]. Finally, it is worth noting another solution of CO_2 limitation resulting from increased load-bearing capacity, higher durability, longer service life, and decreased maintenance costs of concrete structures. This can be achieved in many ways by careful and conscious choice of concrete composition, having in mind particular requirements that the concrete element must meet. It must be noted that for different applications, different properties will be prioritized.

The authors of the article attempted to modify concrete composition to find a more beneficial and effective solution for prefabricated concrete drainage channels in terms of mechanical properties and CO_2 reduction. Concrete drainage channels are usually prefabricated elements used in road construction to drain water excess from streets, pavements, squares, and parking lots to the storm sewage system. Being in contact with water, special attention should be paid to properties such as: tightness, water absorption, and water permeability. In addition, their durability and resistance to unfavorable weather conditions, including large temperature differences, are important. As a result, new, stronger, and more durable solutions are currently being sought to meet sustainable development requirements. To fulfill the requirements referring to enhanced mechanical properties, better durability and CO_2 reduction two changes in the mix design were made. Firstly, metakaolin (MK) was used as a partial replacement for cement to decrease the amount of clinker. Metakaolin is a pozzolanic material formed during a calcination process of kaolinitic clay. As a consequence of MK addition to the concrete mix, the reduction of chloride permeability [7], increase of sulfate [8], and acid attack [9] resistance was noted in other studies. The positive effect of MK incorporation was also recognized in decreasing water absorption, water penetration, porosity [9], sorptivity [10], and shrinkage [11]. All this and additionally considerable enhancement in durability [12] make concrete with MK suitable material for use in structures in contact with water. Moreover, studies also confirmed the increase of

mechanical properties such as compressive [13], flexural, splitting tensile [14], and early age strength [15] when MK was added. The second modification consisted in adding polymer micro- and macro-fibers to the concrete mix. Namely, micro-fibers can bridge micro-cracks and prevent shrinkage, thus the number and width of cracks are smaller [16]. On the other hand, macro-fibers not only bridge macro-cracks, but also increase the toughness, and ductility of concrete [17]. Other properties positively influenced by the addition of polymer fibers are as follows: impact, spalling, freeze-thaw, and abrasion resistance [18]. Furthermore, not only flexural and tensile strength can be improved but water absorption, permeability, and porosity may be decreased when a careful and properly executed mixture design is carried out [18]. It must be mentioned that the addition of fibers can result in the concrete properties enhancement, but only for the optimized fiber dosage, otherwise, the effect will be the opposite. Moreover, undeniably beneficial when it comes to polymer fiber reinforced concrete (PFRC) is its resistance to the negative action of corrosion, unlike steel fiber reinforced concrete or traditional concrete with steel bars. In conclusion, PFRC can be successfully used for elements exposed to water such as concrete drainage channels.

In the experimental program, four concrete mixes were cast: one reference and three with the addition of MK, and polymer micro- and macro-fibers (microPF and macroPF, respectively) differing in fiber type and dosage. The article presents the results of a detailed experimental campaign including a compressive strength test, three- and four-point bending test (3PBT and 4PBT, respectively). The dependencies and correlations between results from tests performed according to EN 14651, RILEM TC 162-TDF, EN 12390-5, and JCI-SF4 were described. Finally, the effectiveness and correctness of formulas presented in the work of Blazy et al. [17] has been confirmed on samples with different composition and fibers.

2. Experimental program

2.1. Materials

Table 1 presents the composition of four Types of concrete mixture: one without and three with fibers. In the study, two Kinds of macroPF (Kind I and II) and one kind of microPF (Kind III) were used. The characterization of used fibers together with the most important properties (fiber length l_f, fiber diameter d_f, fiber slenderness l_f/d_f, fiber tensile strength f_{ft}, and fiber Young's modulus E_f) is shown in Table 2 and pictures in Table 3. Is it worth mentioning that the tested samples can be called hybrid PFRC since they contained both macro- and micro-fibers. Concerning other ingredients, the used cement was CEM II/A-V 42.5 R and in mixes of Type 1, 2, and 3 some part of cement was replaced by metakaolin (MK). Moreover, sand as a fine-grained aggregate and gravel with a maximum diameter of 16 mm as a coarse-grained aggregate were added to the mixture. Water to cement ratio (w/c) was equal to 0.5 for Type 0 and 0.53 for mixes with MK. To ensure proper workability, a superplasticizer was added.

Table 1. Concrete mixture composition (kg/m^3)

Composition	Type 0	Type 1	Type 2	Type 3
CEM II/A-V 42.5 R	370	350	350	350
Sand 0/2 mm	800	800	800	800
Gravel 2/8 mm	525	525	525	525
Gravel 8/16 mm	525	525	525	525
Water	185	185	185	185
Superplasticizer	4.2	4.6	4.6	4.2
Metakaolin MK	–	25	25	25
MacroPF – Kind I	–	2.0	–	–
MacroPF – Kind II	–	–	2.0	2.5
MicroPF	–	1.0	1.0	0.5

Table 2. Characterization of used fibers

Kind I	Kind II	Kind III
$l_f = 42 \pm 1$ mm cross-section = 70×1600 μm	$l_f = 54$ mm $l_f/d_f = 70$	$l_f = 12$ mm $d_f = 0.018$ mm
$f_{ft} = 550$ MPa ±10%	$f_{ft} = 640$ MPa	$f_{ft} = 350 - 400$ MPa
$E_f = 2.8 - 4.0$ GPa	$E_f = 11$ GPa	not known
copolymer PE-PP	polypropylene copolymer	polypropylene

Table 3. Pictures of used fibers

Kind I	Kind II	Kind III
		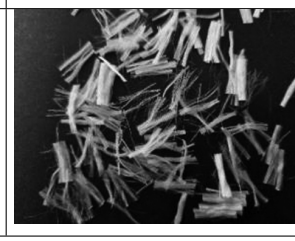

2.2. Sample preparation

Six cubes with dimensions of $150 \times 150 \times 150$ mm and nine beams with dimensions of $150 \times 150 \times 700$ mm were concreted from each series (Fig. 1). The samples were prepared and stored in accordance with respectively: EN 12390-1 [19] and EN 12390-2 [20] in water

at a temperature of 20 ± 2°C until the 28^{th} day [20]. After this period, the samples were stored in air-dry conditions at 20 ± 2°C and 60% humidity until the test date. It must be mentioned that due to the used type of cement and the addition of MK, the samples were tested after 112 (4 × 28) days from casting. Six beams were intended for the 3PBT and three for the 4PBT. As a result, all beams destined for the 3PBT were cut in the middle of the span – 5 mm wide and 25 mm deep along the entire beam width with a diamond saw before the testing day (Fig. 1).

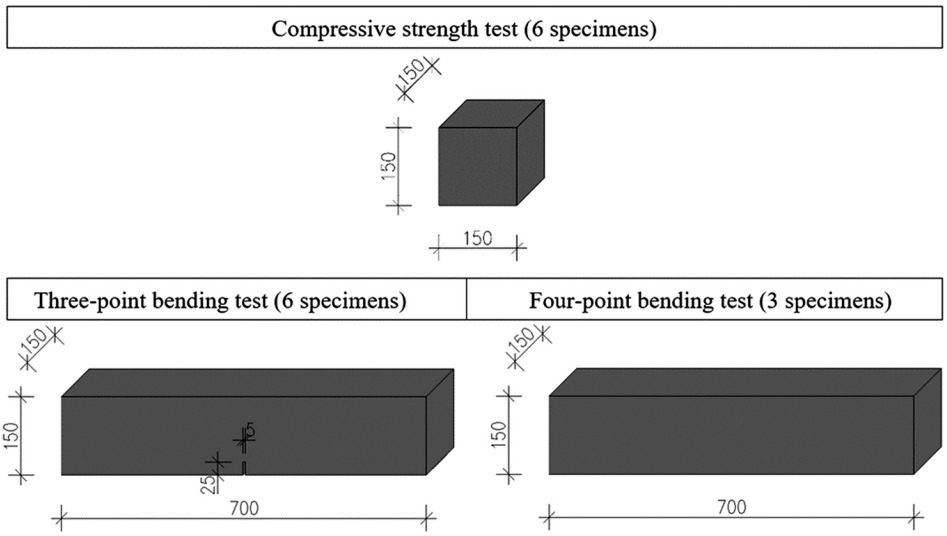

Fig. 1. Experimental program – sample characteristics

2.3. Methodology

The cubes in the compressive strength test were tested in agreement with EN 206 [21] where the stress was increased at a rate of 0.5 MPa/sec. The 3PBT was performed following EN 146 [22] and the 4PBT complied with EN 12390-5 [23]. Fig. 2 and Fig. 3 show the testing set-ups for both bending tests. In the 3PBT and 4PBT, linear variable differential transformers (LVDTs) were installed to measure the beam deflection (δ). They were positioned from both sides thanks to the rigid steel frame attached to the sample. For the analysis, the average from two LVDTs was calculated. Clip gauges to record crack mouth opening displacements (*CMODs*) and crack tip opening displacements (*CTODs*) were installed in the notch area, so only in the 3PBT (Fig. 3b. The span between the supports (l) was equal to 500 and 450 mm for the 3PBT and 4PBT, respectively. The samples were loaded with a force (F) with a constant increment of δ equal to 0.2 mm/min until reaching δ = 5 mm, when the test was stopped. In the 3PBT, the *F–CMOD*, *F–CTOD*, and $F - \delta$ curves were recorded while during the 4PBT just the $F - \delta$ curve. Thanks to the obtained results from the 3PBT it was possible to determine the limit of proportionality $f_{ct,L}^{f}$ (Eq. (2.1)) and residual flexural

tensile strengths: $f_{R,1}$, $f_{R,2}$, $f_{R,3}$, and $f_{R,4}$ (Eq. (2.2)), using the formulas included in [22]. Regarding the 4PBT, standard [23] contains Eq. (2.3) to calculate the flexural tensile strength of concrete. It must be mentioned that only PFRC samples so from Type 1-3 were delivered to the laboratory and only these mixtures were subjected to above mentioned tests.

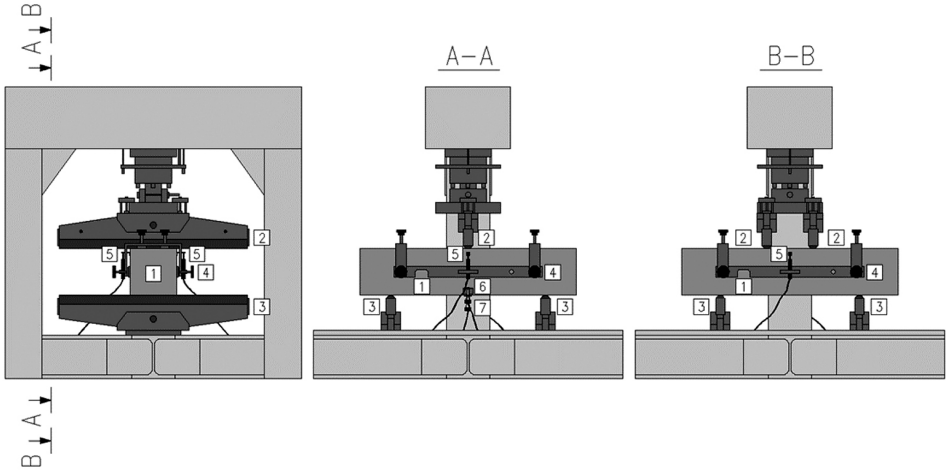

Fig. 2. Testing set-up, where cross-section A-A is for the 3PBT, and cross-section B-B is for the 4PBT: 1 – sample; 2 – loading roller; 3 – supporting roller; 4 – rigid steel frame to install LVDTs; 5 – LVDT to measure δ; 6 – clip gauge to measure *CTOD*; 7 – clip gauge to measure *CMOD*

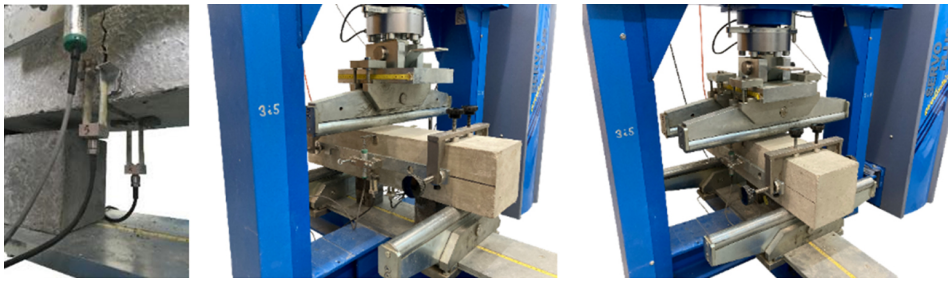

Fig. 3. View of set-ups during the 3PBT (on the left) and 4PBT (on the right)

$$f_{ct,L}^{f} = \frac{3F_L l}{2bh_{sp}^2} \tag{2.1}$$

$$f_{R,j} = \frac{3F_j l}{2bh_{sp}^2} \tag{2.2}$$

where: $f_{ct,L}^{f}$ – limit of proportionality (N/mm^2), $f_{R,j}$ – residual flexural tensile strength corresponding with $CMOD = CMOD_j$ or $\delta = \delta_j$ ($j = 1, 2, 3, 4$) (N/mm^2), F_L – load corresponding to the limit of proportionality (N), F_j – load corresponding to $CMOD = CMOD_j$ or $\delta = \delta_j$ ($j = 1, 2, 3, 4$) (N), l – distance between the supporting rollers (mm)

= 500 mm, b – width of the sample (mm) = 150 mm, h_{sp} – distance between the tip of the notch and the top of the specimen (mm) = 125 mm

$$f_{cf} = \frac{Fl}{d_1 d_2^2} \tag{2.3}$$

where: f_{cf} – flexural tensile strength (N/mm^2), F – load (N), l – distance between the supporting rollers (mm) = 450 mm, d_1 and d_2 – lateral dimensions of the specimen (mm) = 150 and 150 mm, respectively

3. Results and discussion

3.1. Compressive strength test

The compressive strength (f_c) was measured twice: after 56 days and after 112 days (the day of bending tests) from casting. Each time three samples were tested and the mean values for mixtures of Type 1–3 are shown in Table 4. The compressive strength after eight weeks was almost the same for all variants of mixtures regardless of the used fibers and their dosage. The average value of f_c was equal to 44.44 MPa, while the standard deviation was 1.64 MPa, and the coefficient of variation was 3.70%. The class of tested concrete was defined as C30/37 according to the Method A for pre-production when the number of samples is smaller than fifteen [21]. Regarding the later strength, it increased by 32, 27, and 23% for Type 1, 2, and 3, respectively during eight weeks. The average, standard deviation, and coefficient of variation of f_c after 16 weeks from casting was equal to 56.57 MPa, 3.35 MPa, and 5.92%.

Table 4. Results of the compressive strength tests

Type	f_c after 56 days (MPa)	f_c after 112 days (MPa)
1	44.07	58.29
2	44.20	56.06
3	44.90	55.34
Mean	44.44	56.57

3.2. Three-point bending test

3.2.1. Limit of proportionality, equivalent and residual flexural tensile strengths

In the 3PBT six samples for each Type of mixture were tested (numbered from 1 to 6). From *F–CMOD* curves, after the recalculation using Eq. (2.1) and Eq. (2.2), it was possible to obtain $f_{R,j} - CMOD$ graphs shown in Fig. 4 up to $CMOD = 3.5$ mm. It must be mentioned that the sudden drops on the graphs in a post-cracking stage were an evidence of breaking the fibers in the cross-section of the crack. Furthermore, in Table 5 the characteristic values of the 3PBT such as: $f^f_{ct,L}$ and $f_{R,1}$, $f_{R,2}$, $f_{R,3}$, and $f_{R,4}$ are presented.

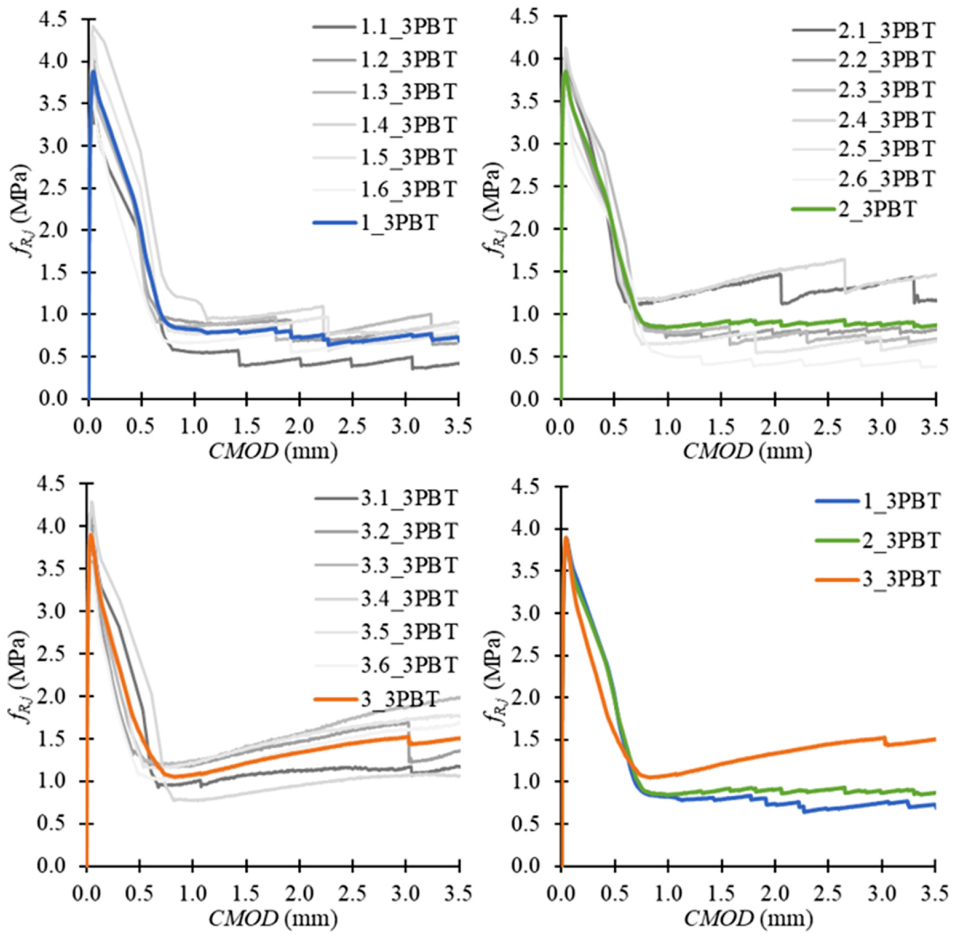

Fig. 4. Results of the 3PBT: $f_{R,j}$ – *CMOD* curves

It was observed that concrete of Type 1 and 2 behaved very similarly which could be related to the same amount of macro- and micro-fibers (2 and 1 kg/m^3, respectively) in the mixture. The only difference in the mix composition between those two series was the kind of macroPF which did not significantly affect the flexural behaviour of samples. In the post-cracking stage the mixture of Type 2 achieved a bit better results since $f_{R,2}$, $f_{R,3}$, and $f_{R,4}$ were 14, 34, and 20% higher than those for Type 1, respectively. It could have been a reason of greater tensile strength f_{ft} and length l_f of fibers of Kind II than Kind I (Table 2). Nevertheless, Type 1–2 after achieving maximum strength were still able to resist further loads while *CMODs* were increasing avoiding in this way the brittle behaviour of concrete. Those two series were characterized by softening behaviour. On the other hand, all samples of Type 3 indicated soft-hardening behaviour. This means that they were able to transform higher and higher forces for increasing values of *CMODs*. The residual

strengths did not reach or surpass the maximum one and this is why it is not possible to classify Type 3 behaviour as a hardening. Nevertheless, the soft-hardening behaviour of Type 3 was a very positive outcome since it is usually attributed to steel fiber reinforced concrete, not PFRC. When comparing with the first two mixtures, the increased dosage of macroPF could have been a result of such an effect. Regarding the residual strength the biggest improvement equal to 19% was distinguished between $f_{R,2}$ and $f_{R,3}$ (Table 5). When it comes to maximum strength the results revealed that the type and amount of PF did not influence this property. The differences in $f^f_{ct,L}$ between Type 1, 2, and 3 were small enough to conclude that the mean flexural tensile strength in the 3PBT was equal to 3.876 MPa. Finally, after the 3PBT beams did not split in half but retained their integrity. Furthermore, all the beams were damaged by a quasi-vertical crack beginning in the notch (Fig. 5).

Fig. 5. Samples 1-4 from concrete Type 1 after the 3PBT – quasi-vertical crack beginning in the notch

Table 5. Results of the 3PBT: limit of proportionality and residual flexural tensile strengths

Type	$f^f_{ct,L}$ (MPa)	$f_{R,1}$ (MPa)	$f_{R,2}$ (MPa)	$f_{R,3}$ (MPa)	$f_{R,4}$ (MPa)
1	3.881	1.979	0.794	0.675	0.726
2	3.848	1.954	0.905	0.904	0.870
3	3.899	1.571	1.212	1.446	1.506

Additionally, RILEM TC 162-TDF [24] proposes the method to define equivalent tensile strengths $f_{eq,2}$ (Eq. (3.1)) and $f_{eq,3}$ (Eq. (3.2)) when the $F-\delta$ curve is known. The results of the 3PBT obtained from LVDTs are presented in Fig. 6 together with the method to calculate $D^f_{BZ,2}$ and $D^f_{BZ,3}$. Furthermore, Table 6 contains the results of $f_{eq,2}$ and $f_{eq,3}$ calculations and previously mentioned $f_{R,1}$ and $f_{R,4}$ for comparison. In this line of research, it can be concluded that values obtained from *F–CMOD* curve did not correspond clearly with data calculated from $F-\delta$ diagram. Namely, for all Types of mixtures, $f_{R,1}$ was greater than $f_{eq,2}$ by 15 to 69%. Considering $f_{R,4}$, only the value for mixture of Type 3 was higher than $f_{eq,3}$ while for the other mixtures $f_{eq,3}$ was more beneficial by around 13.5%. However, in this case, it was possible to define the linear relationship between $f_{R,4}$ and $f_{eq,3}$ (Fig. 7)

with $R^2 = 0.977$. Finally, for Type 1 and 2 the ratio $f_{eq,3}/f_{eq,2}$ and $f_{R,4}/f_{R,1}$ was around 71 and 41%, respectively. For Type 3, which behaved like a soft-hardening material in bending, both equivalent and residual flexural tensile strengths were similar. However, more experimental data are necessary to define unambiguous conclusions about relations between $f_{eq,2}$, $f_{eq,3}$, $f_{R,1}$ and $f_{R,4}$.

$$f_{eq,2} = \frac{3}{2}\frac{D^f_{BZ,2}}{0.5}\frac{l}{bh^2_{sp}} \tag{3.1}$$

$$f_{eq,3} = \frac{3}{2}\frac{D^f_{BZ,3}}{2.5}\frac{l}{bh^2_{sp}} \tag{3.2}$$

where: $f_{eq,2}$ and $f_{eq,2}$ – equivalent tensile flexural strength corresponding with $D^f_{BZ,2}$ and $D^f_{BZ,3}$, respectively (N/mm^2), $D^f_{BZ,2}$ and $D^f_{BZ,3}$ – area under the $F - \delta$ curve representing the contribution of fibers to the energy absorption capacity (N/mm) see Fig. 6.

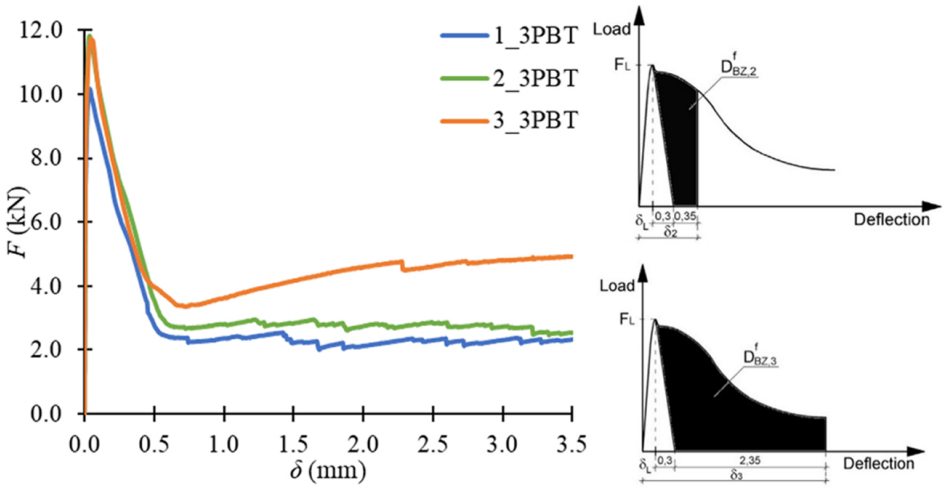

Fig. 6. Results of the 3PBT: $F - \delta$ curves and definition of areas $D^f_{BZ,2}$ and $D^f_{BZ,3}$ areas described in RILEM TC 162-TDF [24] to calculate $f_{eq,2}$ and $f_{eq,3}$, respectively

3.2.2. Fracture energy

The goal of many FRC studies is to define the fracture energy (G_f) which is also called the toughness of concrete. This property is a certain measurement of the ductility provided by the addition of fibers. Within this article, G_f was calculated using Eq. (3.3) limiting it to *CMOD* reaching 3.5 mm. The results of G_f computations based on the *F–CMOD* curves in the 3PBT are presented in Table 7. It can be concluded that concrete of Type 2 and 3 had higher G_f than Type 1 by 5 and 21%, respectively. The greatest improvement was achieved for mixture of Type 3 what is in agreement with the fact that a higher amount of macroPF

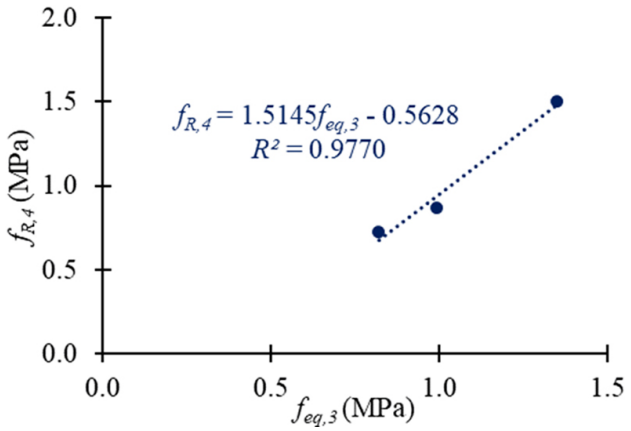

Fig. 7. Relation between $f_{eq,3}$ and $f_{R,4}$ obtained from the experimental data

Table 6. Results of the 3PBT: equivalent flexural tensile strengths calculated from $F - \delta$ curve and residual flexural tensile strengths calculated from *FvCMOD* curve

Type	$D^f_{BZ,2}$ (N·m)	$D^f_{BZ,3}$ (N·m)	$f_{eq,2}$ (MPa)	$f_{eq,3}$ (MPa)	$f_{eq,3}/f_{eq,2}$ (%)	$f_{R,1}$ (MPa)	$f_{R,4}$ (MPa)	$f_{R,4}/f_{R,1}$ (%)	$f_{R,1}/f_{eq,2}$ (%)	$f_{R,4}/f_{eq,3}$ (%)
1	1.825	6.402	1.168	0.819	70	1.979	0.726	37	169	89
2	2.167	7.758	1.387	0.993	72	1.954	0.870	45	141	88
3	2.126	10.550	1.361	1.350	99	1.571	1.506	96	115	111

results in more enhanced toughness as long as the concrete mixture is properly designed (workability does not deteriorate).

$$G_f = \frac{W_0 + mg\delta}{b(h - a_0)} \tag{3.3}$$

where: G_f – fracture energy (N/m), W_0 – area under the *F-CMOD* curve until *CMOD* reaching 3.5 mm (N·m), m– sample mass between the supporting rollers (kg), g – gravitational acceleration = 9.81 N/kg (N/kg), δ – *CMOD* when the F drops to 0 – herein assumed 3.5 mm (m), b – sample width = 150 mm (m), h – sample height = 150 mm (m), a_0 – notch height = 25 mm (m)

Table 7. Fracture energy in the 3PBT

Mixture type	W_0 (N·m)	m (kg)	G_f (N/m)
1	12.140 (100%)	25.695	1118 (100%)
2	13.235 (109%)	25.830	1179 (105%)
3	16.442 (135%)	25.786	1349 (121%)

3.2.3. Relation between δ, *CMOD*, and *CTOD*

EN 14651 [22] presents the formula to relate δ and *CMOD* (Eq. (3.4)). However, it must be mentioned that the standard is designed for metallic fiber reinforced concrete. As a result, the authors of this article examined the validity of using this formula for samples with non-metallic fibers. Furthermore, in work of Blazy et al. [17], a new formula especially destined for PFRC was proposed (Eq. (3.5)). The goal was to check the correctness and effectiveness of Eq. (3.5) based on tests conducted on samples with different composition and fibers.

$$\delta = 0.850CMOD + 0.04 \tag{3.4}$$

$$\delta = 0.734CMOD + 0.0065 \tag{3.5}$$

During the analysis, the average relationship between *CMOD* from sixteen samples subjected to the 3PBT was defined. It must be mentioned that in total eighteen samples were tested (six from each type). However, specimens 1.2 and 1.4 were eliminated from the analysis since the steel frame, which mounted LVDTs, was shifted at the beginning of the 3PBT. Based on the findings shown in Fig. 8, it was noted that the formula presented in EN 14651 [22] noticeably differed from the experimental *CMOD*-δ curve. A significantly better fit was obtained for the equation found by Blazy et al. in [17]. Considering this, the effectiveness and correctness of Eq. (3.5) was confirmed on samples with different composition and fibers. It is a reason to assume that Eq. (3.5) is more suitable for non-metallic FRC than Eq. (3.4) designed for metallic FRC and can be successfully used for the calculation of PFRC.

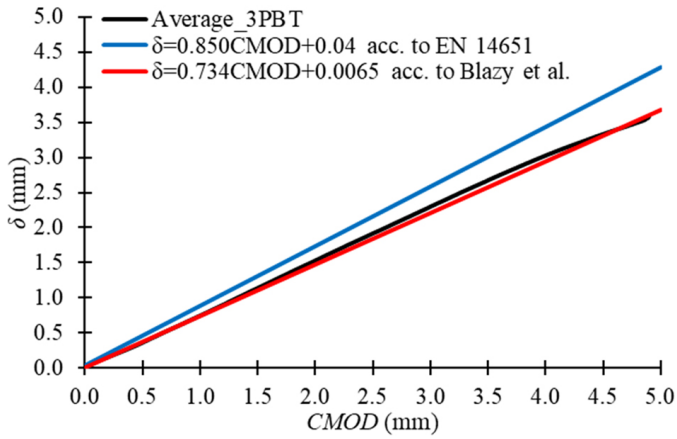

Fig. 8. *CMOD*-δ diagram for experimentally tested PFRC with the formula presented in EN 14651 [22] and in the article of Blazy et al. [17]

In this line of research also other dependencies presented in the work [17] were checked. The relation between *CMOD* and *CTOD* was introduced there by Eq. (3.6). Herein, all eighteen samples were considered while the average curve was defined. Results revealed

(Fig. 9) that again formula proposed by Blazy et al. [17] estimated the experimental results quite well and with big accuracy.

$$CTOD = 0.7685CMOD + 0.0523 \tag{3.6}$$

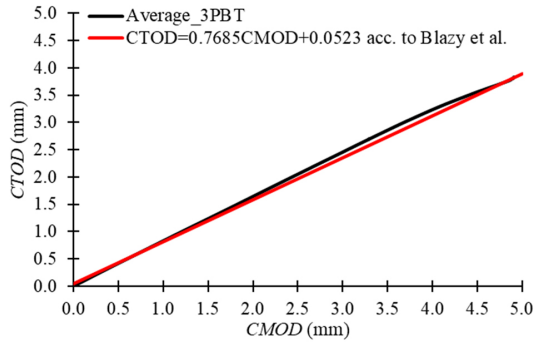

Fig. 9. *CMOD-CTOD* diagram for experimentally tested PFRC with the formula presented in the article of Blazy et al. [17]

Finally, the last relationship possible to estimate from the carried-out tests was defined. Eq. (3.7) shows the dependency between *CTOD* and δ proposed in [17]. As it was mentioned before, the steel frame, which mounted LVDTs, was shifted while testing samples 1.2 and 1.4 so here sixteen curves were used to evaluate the mean one. From Fig. 10 it can be concluded that the Blazy et al. proposal can successfully predict with good precision the values of *CTODs* knowing δ and vice versa.

$$\delta = 0.954CTOD - 0.0434 \tag{3.7}$$

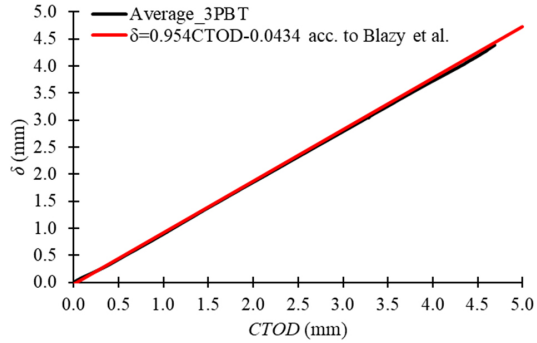

Fig. 10. *CTOD-*δ diagram for experimentally tested PFRC with the formula presented in the article of Blazy et al. [17]

3.3. Four-point bending test

3.3.1. Maximum flexural tensile strength

In the 4PBT three samples (numbered 7, 8, and 9) were tested for each Type of mixture. From $F - \delta$ curves using Eq. (2.3), $f_{cf} - \delta$ graphs were obtained and are shown in Fig. 11. Similarly, as in the 3PBT, the sudden drops on the curves in a post-cracking stage represented the breaking of PF in the cross-section of the crack. Furthermore, in Table 8 the maximum flexural tensile strengths $f_{cf,\max}$ compared with the limits of proportionality $f^{f}_{ct,L}$ from the 3PBT are presented.

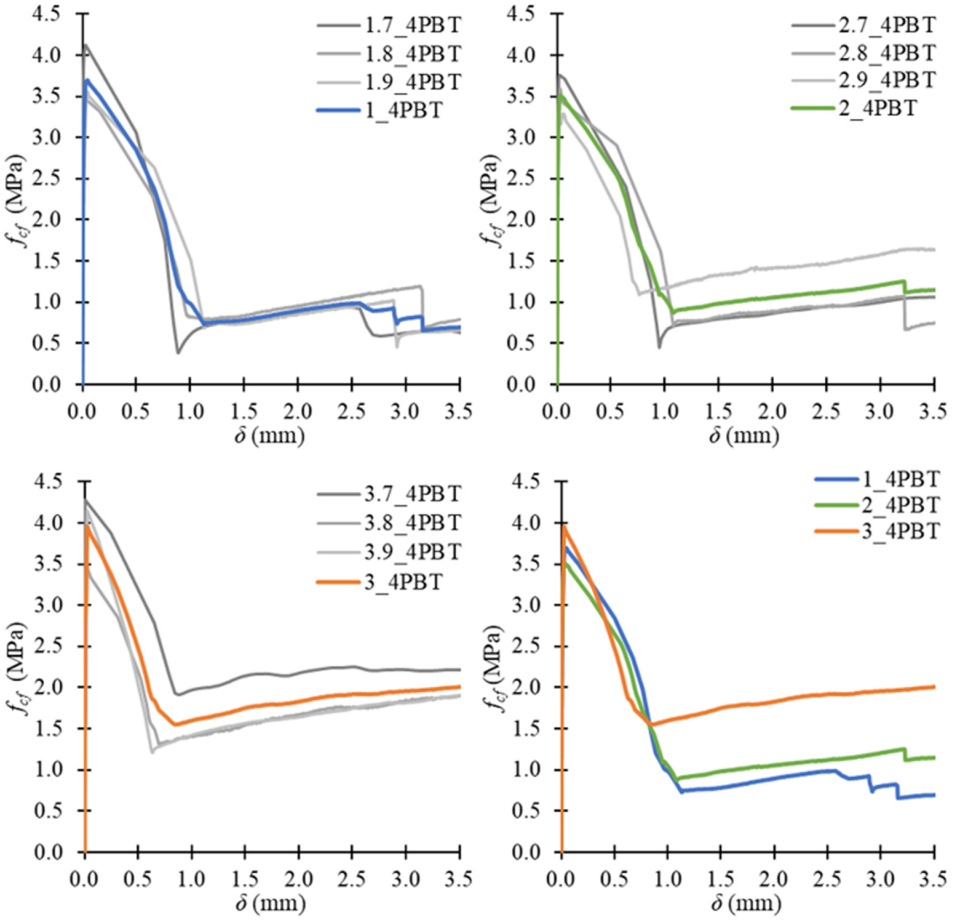

Fig. 11. Results of the 4PBT: $f_{cf} - \delta$ curves

The behaviour of mixtures of Type 1, 2, and 3 in the 4PBT was very similar to the one in the 3PBT, which additionally confirmed the correctness of performed tests. Namely, there was no big difference between the $f_{cf} - \delta$ curves of Type 1 and 2, which could have

Table 8. Results of the 4PBT: maximum flexural tensile strength together with the limit of proportionality from the 3PBT

Type	$f_{cf,\max}$ (MPa)	$f^f_{ct,L}$ (MPa)	$f^f_{ct,L}/f_{cf,\max}$ (%)
1	3.696	3.881	105
2	3.515	3.848	109
3	3.957	3.899	99
Mean	3.723	3.876	104

been attributed to the fact that only the type of macro-fiber varied between those two series. In the post-cracking stage, after achieving δ equal to around 1 mm, Type 1 had a lower load-bearing capacity. It could have been a reason of smaller f_{ft} and l_f of fibers of Kind I when comparing with Kind II (Table 2). It must be mentioned that Type 3 achieved the highest $f_{cf,\max}$ when compared with other mixtures. Furthermore, due to the addition of PF, all tested samples were characterized by ductile behaviour since there were able to resist some forces while the deflection of the beam was increasing even though the maximum strength was reached. Additionally, samples of Type 3 showed the softening-hardening behaviour in the 4PBT like it was noticed also in the 3PBT. When comparing with the first two mixtures, the increased dosage of macroPF could have been a result of such an effect. Similarly, to the 3PBT, after the 4PBT beams did not break completely and in all the samples, the quasi-vertical crack appeared between the upper support (Fig. 12).

Fig. 12. Samples 7-9 from concrete of Type 1 and 2 after the 4PBT – quasi-vertical crack between the upper supports

3.3.2. Fracture energy

The 4PBT was carried out according to EN 12390-5 [23] but it also fulfilled the requirements of the Japanese standard JCI-SF4 [25] (for example: sample geometry, support and force arrangement). Due to this, it was decided to calculate the work T_b required to obtain a beam deflection equal to $^1/_{150}$ of its span. Namely, the area under the $F - \delta$ curve was defined limiting it to δ reaching 3 mm. Knowing the value of T_b, it was possible to assess the equivalent flexural tensile strength f_{eq} applying Eq. (3.8) included in [25]. It is noteworthy, that f_{eq} value is used to calculate the fracture toughness index R_e, which occurs in some formulas while designing FRC elements (Eq. (3.9)). Defining R_e allows using the additional load-bearing capacity obtained from the incorporation of fibers. For example, the 3^{rd} edition of the Technical Report 34 [26] about concrete industrial ground floors allows to include the beneficial effect of fibers while calculating the upper/positive bending moment M_p. However, the R_e value must be at least equal to 0.30.

$$f_{\text{eq}} = \frac{T_b l}{\delta_{tb} b h^2} \tag{3.8}$$

where: f_{eq} – equivalent flexural tensile strength (N/mm^2), T_b – work required to obtain a beam deflection equal to $^1/_{150}$ of l (Nmm), l – span between the bottom supports (mm), δ_{tb} – deflection equal to $^1/_{150}$ of l (l = 450 mm so δ_{tb} = 450/150 = 3 mm) (mm), b – sample width = 150 mm (mm), h – sample height = 150 mm (mm)

$$R_e = 100 \frac{f_{\text{eq}}}{f_{ctm,fl}} \tag{3.9}$$

where: R_e – fracture toughness index (%), $f_{ctm,fl}$ – mean flexural tensile strength (N/mm^2)

Firstly, the area under the $F - \delta$ curve for each Type of mixture was defined until reaching δ = 3 mm, then T_b, f_{eq}, and R_e were calculated (Fig. 13). It must be mentioned that as the $f_{ctm,fl}$, the experimental values of $f_{cf,\max}$ from the 4PBT were assumed. The smallest f_{eq} was achieved for mixture of Type 1, and then 5 and 42% higher values were obtained by Type 2 and 3, respectively when compared with the first mix. The R_e was

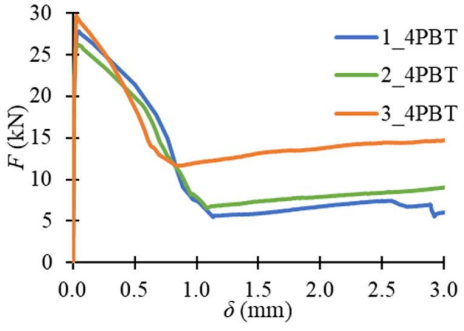

Type	1	2	3
T_b (Nm)	32.457	34.144	46.169
$f_{ctm,fl} = f_{cf,\max}$ (MPa)	3.696	3.515	3.957
f_{eq} (MPa)	1.443	1.518	2.052
R_e (%)	39	43	52

Fig. 13. Results of the 4PBT: $F - \delta$ curves to define T_b, f_{eq}, and R_e according to JCI-SF4 [25]

equal to 39, 43, and 52% for Type 1, 2, and 3. It can be concluded that the most beneficial effect on the load-bearing capacity of the structural element would have been achieved if concrete mixture of Type 3 was used so with 2.5 kg/m^3 of macroPF and 0.5 kg/m^3 of microPF. Moreover, an attempt was made to find the correlation between the f_{eq} and $f_{\mathrm{eq},3}$ or $f_{R,4}$ obtained from the experimental data. It was concluded that the linear relation existed between f_{eq} and $f_{\mathrm{eq},3}$ as well as between f_{eq} and $f_{R,4}$ (Fig. 14). However, further research and more experimental data are necessary to confirm these dependencies.

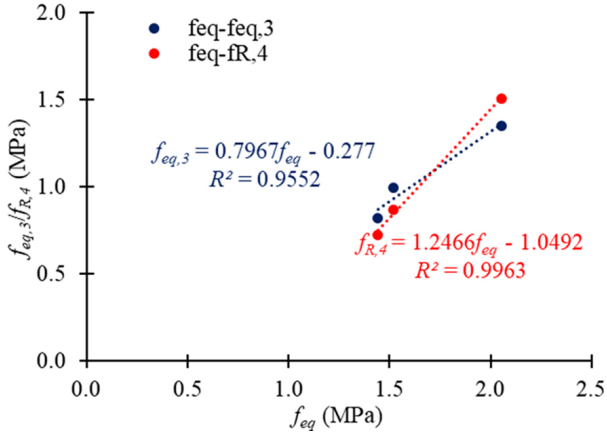

Fig. 14. Relation between f_{eq} and $f_{\mathrm{eq},3}$ or $f_{R,4}$ obtained from the experimental data

4. Conclusions

The most relevant conclusions of the current study are the following:

– The addition of polymer fibers did not influence the compressive strength of samples. The average value of f_c was equal to 44.44 MPa and the concrete class was defined as C30/37 for all tested Types of mixtures.
– In the 3PBT and 4PBT concrete Type 1 and 2 behaved very similarly which could be related to the same amount of macro- and micro-fibers. Those two series were characterized by softening behaviour. In the post-cracking stage Type 2 achieved a bit greater residual flexural tensile strengths than Type 1. It could have been a reason of greater tensile strength and length of fibers added to the mixture Type II than to the mixture Type I. On the other hand, all samples of Type 3 indicated soft-hardening behaviour. The increased dosage of macro-fibers in mixture Type 3 could have been a result of such an effect.
– The maximum flexural tensile strength in the 3PBT and 4PBT was not influenced by the type and amount of polymer fibers and the mean value was equal to $f^f_{ct,Lv} = 3.876$ and $f_{cf,\max} = 3.723$ MPa, respectively.
– In the 3PBT, residual flexural tensile strengths $f_{R,j}$ obtained according to EN 14651 did not correspond clearly with equivalent flexural tensile strengths $f_{\mathrm{eq,j}}$ calculated in

compliance with RILEM TC 162-TDF. However, it was possible to define the linear relationship between $f_{R,4}$ and $f_{eq,3}$: $f_{R,4} = 1.5145 f_{eq,3} - 20.5628$.
- The fracture energy G_f in the 3PBT for mixtures of Type 1, 2, and 3 was equal to 1118 (100%), 1179 (105%), and 1349 (121%) N/m, respectively.
- The effectiveness and correctness of equations presented in the work of Blazy et. al [17] for the 3PBT: $\delta = 0.734 CMOD + 0.0065$, $CTOD = 0.7685 CMOD + 0.0523$, and $\delta 0.954 CTOD - 0.0434$ was confirmed on samples with different composition and fibers.
- Based on the 4PBT, the equivalent flexural tensile strength f_{eq} according to JCI-SF4 was calculated for each Type of mixture. The linear relation was defined between f_{eq} and $f_{eq,3}$: $f_{eq,3} = 0.7967 f_{eq} - 0.277$ as well as between f_{eq} and $f_{R,4}$: $f_{R,4} = 1.2466 f_{eq} - 1.0492$.
- The fracture toughness index R_e for the 4PBT was equal to 0.39, 0.43, and 0.52 for Type 1, 2, and 3.

Acknowledgements

The experimental campaign and publication of this article was financially supported by the company *ASTRA Technologia Betonu*.

References

[1] J. Blazy, R. Blazy, and Ł. Drobiec, "Glass fiber reinforced concrete as a durable and enhanced material for structural and architectural elements in smart city – a review", *Materials*, vol. 15, no. 8, art. no. 2754, 2022, doi: 10.3390/ma15082754.

[2] A. Sobotka, K. Linczowski, and A. Radziejowska, "Determinants of substitution in the environmental aspect of sustainable construction", *Archives of Civil Engineering*, vol. 69, no. 1, pp. 163–179, 2023, doi: 10.24425/ace.2023.144166.

[3] S.K. Seyedebrahimi, A. Mirjalili, and A. Sadeghian, "Identification and prioritization of factors influencing the increase in construction costs of building investments using factor analysis", *Archives of Civil Engineering*, vol. 67, no. 3, pp. 705–722, 2021, doi: 10.24425/ace.2021.138079.

[4] Instytut Techniki Budowlanej ITB, "Environmental Product Declaration Type III ITB – Cements CEM I, CEM II, CEM III, CEM IV, CEM V produced in Poland". 2020. [Online]. Available: https://www.polskicement.pl/wp-content/uploads/2021/12/Deklaracja-srodowiskowa-ENG.pdf.

[5] Polish Cement Association, "Spajamy Europejski Zielony Ład – Osiągnięcie neutralności emisyjnej w łańcuchu wartości cementu i betonu do roku 2050". 2020. [Online]. Available: https://www.polskicement.pl/wp-content/uploads/2020/05/SPC-CEMBUREAU-2050-ROADMAP_PL.pdf.

[6] Polish Cement Association, *Concrete a low emission building material*. Kraków: Polish Cement Association, 2021.

[7] A.A. Abouhussien and A.A.A. Hassan, "Optimizing the durability and service life of self-consolidating concrete containing metakaolin using statistical analysis", *Construction and Building Materials*, vol. 76, pp. 297–306, 2015, doi: 10.1016/j.conbuildmat.2014.12.010.

[8] M.A. Chandak and P.Y. Pawade, "Influence of metakaolin in concrete mixture: a review", *The International Journal of Engineering and Science*, pp. 37–41, 2018.

[9] G.L. Thankam and N.T. Renganathan, "Ideal supplementary cementing material – Metakaolin: a review", *International Review of Applied Sciences and Engineering*, vol. 11, no. 1, pp. 58–65, 2020, doi: 10.1556/1848.2020.00008.

[10] E. Güneyisi, M. Gesoglu, Z. Algin, and K. Mermerdaş, "Optimization of concrete mixture with hybrid blends of metakaolin and fly ash using response surface method", *Composites Part B: Engineering*, vol. 60, pp. 707–715, 2014, doi: 10.1016/j.compositesb.2014.01.017.

[11] A.M. Matos, L. Maia, S. Nunes, and P. Milheiro-Oliveira, "Design of self-compacting high-performance concrete: Study of mortar phase", *Construction and Building Materials*, vol. 167, pp. 617–630, 2018, doi: 10.1016/j.conbuildmat.2018.02.053.

[12] B. B. Sabir, S. Wild, and J. Bai, "Metakaolin and calcined clays as pozzolans for concrete: a review", *Cement & Concrete Composites*, vol. 23, no. 6, pp. 441–454, 2001, doi: 10.1016/S0958-9465(00)00092-5.

[13] H.S. Wong and H.A. Razak, "Efficiency of calcined kaolin and silica fume as cement replacement material for strength performance", *Cement and Concrete Research*, vol. 35, no. 4, pp. 696–702, 2005, doi: 10.1016/j.cemconres.2004.05.051.

[14] S. Issac and A. Paul, "A literature review on the effect of metakaolin and fly ash on strength characteristics of concrete", *International Journal Of Advance Research And Innovative Ideas In Education*, vol. 4, no. 2, pp. 6–11, 2018, doi: 16.0415/IJARIIE-7446.

[15] V. Shah and S. Bishnoi, "Use of marble dust as clinker replacement in cements", in *Advances in structural engineering*, V. Matsagar, Ed. Springer India, 2015, pp. 1717–1724, doi: 10.1007/978-81-322-2187-6_130.

[16] Ł. Drobiec and J. Blazy, "Współczesne niemataliczne zbrojenie rozproszone stosowane w konstrukcjach betonowych", *Izolacje*, vol. 61, no. 5, pp. 70–84, 2020.

[17] J. Blazy, Ł. Drobiec, and P. Wolka, "Flexural tensile strength of concrete with synthetic fibers", *Materials*, vol. 14, no. 16, art. no. 4428, 2021, doi: 10.3390/ma14164428.

[18] J. Blazy and R. Blazy, "Polypropylene fiber reinforced concrete and its application in creating architectural forms of public spaces", *Case Studies in Construction Materials*, vol. 14, art. no. e00549, 2021, doi: 10.1016/j.cscm.2021.e00549.

[19] EN 12390-1:2021 Testing hardened concrete – Part 1: Shape, dimensions and other requirements for specimens and moulds.

[20] EN 12390-2:2019 Testing hardened concrete – Part 2: Making and curing specimens for strength tests.

[21] EN 206:2013+A2:2021 Concrete – Specification, performance, production and conformity.

[22] EN 14651+A1:2007 Test method for metallic fibre concrete – Measuring the flexural tensile strength (limit of proportionality (LOP), residual).

[23] EN 12390-5:2009 Testing hardened concrete – Part 5: Flexural strength of test specimens.

[24] "RILEM TC 162-TDF: Test and design methods for steel fibre reinforced concrete, final recommendations", *Materials and Structures*, vol. 35, no. 9, pp. 579–582, 2002.

[25] JSCE-SF4 Methods of tests for flexural strength and flexural toughness of fiber reinforced concrete. 1984.

[26] The Concrete Society, *Technical Report 34. Concrete industrial ground floors. A guide to design and construction*, 3rd ed. The Concrete Society, 2003.

Właściwości mechaniczne betonu zbrojonego włóknami polimerowymi w świetle różnych norm

Słowa kluczowe: fibrobeton, korytka ściekowe, test trzy-punktowego zginania, test cztero-punktowego zginania, włókna polimerowe

Streszczenie:

Obecnie coraz większy nacisk kładzie się na zrównoważony rozwój produkcji i konsumpcji betonu. Wynika to z faktu, że produkcja cementu odpowiada za około 5% światowej emisji CO_2. W celu znalezienia korzystniejszego rozwiązania dla prefabrykowanych korytek ściekowych uwzględniającego zalecenia redukcji CO_2 oraz polepszenia właściwości mechanicznych i trwałościowych, zmodyfikowano skład mieszanki betonowej. Zastosowano metakaolin (MK) jako częściowy zamiennik

cementu w celu zmniejszenia ilości klinkieru oraz dodano do mieszanki betonowej włókna polimerowe (PF). W artykule przedstawiono wyniki szczegółowej kampanii eksperymentalnej obejmującej testy wytrzymałości na ściskanie, trzy- i czteropunktowe zginanie (odpowiednio testy 3PBT i 4PBT) betonu zbrojonego włóknami polimerowymi (PFRC) z dodatkiem MK. Badania obejmowała trzy Typy mieszanek betonowych różniące się ilością oraz typem zastosowanych PF. Każda mieszanka betonowa zawierała zarówno mikro- jak i makro-włókna polimerowe (odpowiednio mikroPF i makroPF), zatem można je było nazwać hybrydowymi PFRC. Typ 1 i 2 zawierał 2,0 kg/m^3 makroPF i 1,0 kg/m^3 mikroPF, różnica polegała na rodzaju włókna makro. Natomiast do Typu 3 dodano 2,5 i 0,5 kg/m^3 makro- i mikroPF, odpowiednio, rodzaj włókien byłtaki sam jak w Typie 2. Wykonano sześć kostek o wymiarach 150 × 150 × 150 mm do testów wytrzymałości na ściskanie zgodnych z normą EN 206; sześć belek o wymiarach 150 × 150 × 700 mm do testów 3PBT zgodnych z normą EN 14651, które później nacięto w środku rozpiętości oraz trzy belki o wymiarach 150 × 150 × 700 mm do testów 4PBT zgodnych z normą EN 12390-5. W wyniku badań stwierdzono, że dodatek PF do mieszanki betonowej nie wpłynął na wytrzymałość na ściskanie betonu. Średnia wytrzymałość na ściskanie f_c wyniosła 44,44 MPa, a klasę betonu dla wszystkich badanych Typów betonu określono jako C30/37. W przypadku testów 3PBT i 4PBT betony Typu 1 i 2 zachowywały się bardzo podobnie, co mogło wynikać z takiej samej ilości makro- i mikro-włókien w betonie. Te dwie serie charakteryzowały się zachowaniem osłabiającym (z ang. *softening behaviour*). W fazie po zarysowaniu Typ 2 przyjmował nieco większe wartości resztkowych wytrzymałości na rozciąganie przy zginaniu niż Typ 1. Przyczyną mogła być większa długość i wytrzymałość na rozciąganie włókien zastosowanych w betonie Typu 2 w porównaniu do tych dodanych do mieszanki Typu 1. Dodatkowo, wszystkie próbki Typu 3 wykazywały zachowanie osłabiające ze wzmocnieniem (z ang. *soft-hardening behaviour*). Powodem takiego efektu mogła być zwiększona ilość makroPF w mieszance Typu 3 (2,5 kg/m^3 zamiast 2,0 kg/m^3 jak w Typie 1 i 2). Zwykle tego rodzaju zachowanie zauważa się dopiero dla betonów zbrojonych włóknami stalowymi, rzadziej dla PFRC. Zaobserwowano również, że na maksymalną wytrzymałość na rozciąganie przy zginaniu w testach 3PBT i 4PBT nie miałwpływu ani rodzaj ani ilość włókien, a średnia wartość wyniosła odpowiednio $f^f_{ct,L} = 3,876$ i $f_{cf,\max} = 3,723$ MPa. Ponadto, w teście 3PBT resztkowe wytrzymałości na rozciąganie przy zginaniu $f_{R,j}$ uzyskane zgodnie z EN 14651 nie odpowiadały dokładnie równoważnej wytrzymałości na rozciąganie przy zginaniu $f_{\mathrm{eq,j}}$ obliczonej zgodnie z RILEM TC 162-TDF. Udało się jednak określić zależność liniową między $f_{R,4}$ a $f_{\mathrm{eq},3}$: $f_{R,4} = 1,5145 f_{\mathrm{eq},3} - 0,5628$. Określono również energię pękania G_f w teście 3PBT dla mieszanek Typu 1, 2 i 3, która wynosiła odpowiednio 1118 (100%), 1179 (105%) i 1349 (121%) N/m. Na koniec analiz testów 3PBT, potwierdzono skuteczność i poprawność wzorów przedstawionych w pracy Blazy i in. *Flexural tensile strength of concrete with synthetic fibers* na próbkach o innym składzie materiałowym i z innymi włóknami. Wzory te dotyczyły następujących zależności: $\delta = 0,734 CMOD + 0,0065$, $CTOD = 0,7685 CMOD + 0,0523$ oraz $\delta = 0,954 CTOD - 0,0434$. Analizy wykazało także większą dokładność wzoru $\delta = 0,734 CMOD + 0,0065$ dla PFRC niż wzór $\delta = 0,850 CMOD + 0,04$ zaproponowany w normie EN 14651, która przeznaczona jest dla fibrobetonów z włóknami metalicznymi. Natomiast w oparciu o testy 4PBT obliczono równoważną wytrzymałość na rozciąganie przy zginaniu f_{eq} zgodnie z japońską normą JCI-SF4 dla każdego Typu betonu. W wyniku obliczeń określono zależność liniową między f_{eq} i $f_{\mathrm{eq},3}$: $f_{\mathrm{eq},3} = 0,7967 f_{\mathrm{eq}} - 0,277$ oraz między f_{eq} i $f_{R,4}$: $f_{R,4} = 1,2466 f_{\mathrm{eq}} - 1,0492$. Na podstawie wartości f_{eq} policzono wskaźnik odporności na pękanie R_e, który wynosił 0,39, 0,43 i 0,52 dla betonu Typu 1, 2 i 3.

Received: 2023-08-04, Revised: 2023-09-05